Robust quantum coherence above the Fermi sea

S. Tewari, P. Roulleau, C. Grenier, F. Portier, A. Cavanna, U. Gennser, D.
Mailly, P. Roche

Robust quantum coherence above the Fermi sea

S. Tewari,[1,2] P. Roulleau,[1] C. Grenier,[3] F. Portier,[1] A. Cavanna,[2] U. Gennser,[2] D. Mailly,[2] and P. Roche[1,*]

[1]*Nanoelectronic Group, SPEC, CEA, CNRS, Université Paris-Saclay, F-91191 Gif-sur-Yvette, France*
[2]*Phynano Team, Laboratoire de Photonique et Nanostructures, CNRS, Route de Nozay, F-91460 Marcoussis, France*
[3]*Institute for Quantum Electronics, ETH Zurich, CH-8093 Zurich, Switzerland*

In this paper we present an experiment where we measured the quantum coherence of a quasiparticle injected at a well-defined energy above the Fermi sea into the edge states of the integer quantum Hall regime. Electrons are introduced in an electronic Mach-Zehnder interferometer after passing through a quantum dot that plays the role of an energy filter. Measurements show that above a threshold injection energy, the visibility of the quantum interferences is almost independent of the energy. This is true even for high energies, up to 130 μeV, well above the thermal energy of the measured sample. This result is in contradiction with our theoretical predictions, which instead predict a continuous decrease of the interference visibility with increasing energy.

A new type of quantum device, relying on the one-dimensional edge states of the quantum Hall regime, where electrons mimic the photon trajectory of a laser beam, has opened a route towards electron quantum optics and the manipulation of single electron excitations [1–3]. Pauli statistics and interactions provide new ingredients for the physics of the electrons which are not relevant for photons. For example, when electrons are injected above the Fermi sea, it is fundamental to understand how their phase coherence will be affected by the injection energy. We explore this issue by first using a quantum dot to inject the carriers at a controllable energy into an edge state. Then an electronic Mach-Zehnder interferometer is used to monitor the quantum coherence of the electronic quasiparticle. We find that above a certain threshold, the coherence is energy independent; it is even preserved at energies 50 times larger than the electronic temperature. This is remarkable, since from simple considerations based on Fermi's golden rule, one would expect that the relaxation rate increases with the injection energy, thus reducing quantum coherence. Indeed, our simulations using recent theories [4] predict a continuous trend of increasing relaxation. While the origin of this coherence robustness remains unidentified, it has a significant bearing for the implementation of quantum information encoded in electron trajectories [5–8].

The edge states used in this new type of device for electronic quantum optics are obtained by applying a high magnetic field perpendicular to a high mobility two-dimensional (2D) electron gas. When the number of electrons per quantum of flux (the filling factor) is an integer, the transport occurs through one-dimensional channels located at the edge of the sample. The electron motion in these wires is chiral: The electrons drift in one direction with a speed of the order of 10^4–10^6 ms^{-1} [9,10], thus compensating the confining electric field with the Lorentz force. Much recent progress has been made in the understanding of decoherence mechanisms and the energy exchanges in the integer quantum Hall regime at a filling factor of 2. In this regime, there are two parallel, adjacent channels at each edge in the sample. The Coulomb interaction has been shown to play a key role in these systems:

(i) The quantum coherence at finite temperature is limited by the thermal charge noise of the environment [11,12]; (ii) there is an energy relaxation in out-of-equilibrium edge states and an energy transfer between the two edge states [13]; and (iii) the visibility of quantum interferences in electronic Mach-Zehnder interferometers exhibits a side lobe structure at finite bias, which is explained by a beating effect between a neutral and a charged excitation shared by the two edge states [4,14–17]. Here, we inject a quasiparticle at a well-defined energy above the Fermi sea into an edge channel. We then explore to which extent such a single charge behaves as a free noninteracting particle in this interacting quantum system, thus directly probing the validity of the Landau's Fermi liquid picture [18,19]. While extensively studied in diffusive quantum conductors, this question has yet to be addressed experimentally for the case of one-dimensional chiral conductors. We note, however, that this is a key point for quantum information experiments using electrons transported through edge channels. Experimentally, we use a quantum dot (QD) as an energy filter, and a Mach-Zehnder interferometer to probe the injected quasiparticle's loss of phase coherence.

The QD consists of two quantum point contacts (QPCs) and a plunger gate (see Fig. 1). Figure 2(a) shows a 2D plot of the transmission probability through the dot as a function of the drain-source bias and the plunger gate voltage V_P. The transmission probability is defined as dI_T/dI_0, where I_T is the transmitted current through the QD and I_0 is the impinging current. From this measurement we deduce the lever arm of the plunger gate $\alpha = d\epsilon/d(eV_P) = 1.46 \times 10^{-4}$, where ϵ is the QD energy. As an example, Fig. 3 (top graph) displays the current I_T as a function of V_P. It is clear that I_T is almost constant for energies varying between 0 and eV_{DS}. This signals an absence of excited states for this particular tuning of the quantum dot. We deduced an electronic temperature of 31 ± 1 mK by fitting the resonance of the transmission probability [see Fig. 2(b)] as a function of V_P with $dI_T/dI_0 \propto$ cosh$^{-2}(\delta/2k_B T)$ [20], where $\delta = \alpha(eV_P - eV_{P_0})$ is the energy difference between the QD energy level and the Fermi level, and V_{P_0} is the plunger gate voltage which maximizes the conductance. Indeed, the intrinsic width of the energy filter is much smaller than the electronic temperature. In practice, the presence of excited states in the dot limited the energy
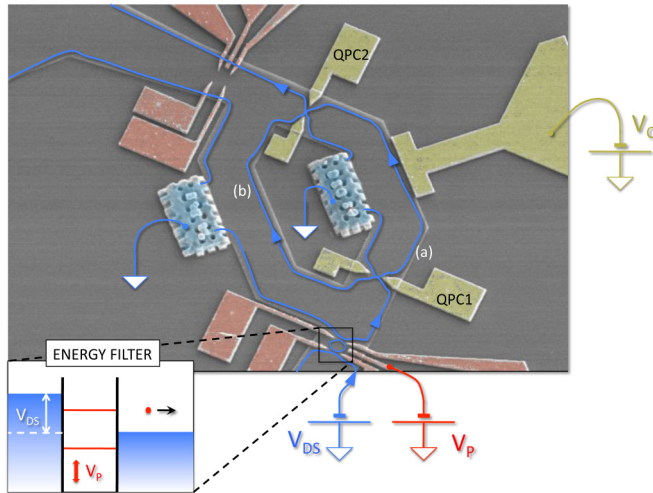
*patrice.roche@cea.fr

FIG. 1. Measured device. Colorized scanning electron microscope view of the sample before the final fabrication step in which the gates and ohmic contacts are connected to larger connecting pads. The sample consists of a quantum dot in series with an electronic Mach-Zehnder interferometer (MZI). The quantum point contacts (QPCs) and gates controlling the dot are in red while those controlling the MZI are in yellow. QPC1 and QPC2 serve as the two beam splitters of the MZI. Note the small ohmic contacts in blue connected to the ground, which prevents spurious quantum interferences inside the interferometer. The chiral trajectory of the excitations in the outer edge state is schematically represented in blue, and the quantum interference takes place between the trajectories (a) and (b). The mesa is 1.2 μm wide, each arm of the Mach-Zehnder interferometer is 7.2 μm long, and the distance between the dot (the energy filter) and the MZI is 2.8 μm. V_P is the potential applied on the plunger gate of the dot, allowing a control of the relative position of the energy levels of the dot compared to the Fermi level. The quantum interferences in the MZI are revealed by sweeping the gate voltage V_C, which modifies the trajectory length difference between (a) and (b).

range we explored to 120 μeV, close to the addition energy estimated to be of the order of 150 μeV [see the Supplemental Material (SM) [21]].

Once the QD is characterized, we measure the current through the whole system, constituted by the QD in series with the MZI, and operated in its optimal parameter regime for maximum visibility (see SM [21]). Probing the decoherence at finite energy is simply realized by measuring the relative amplitude of the current oscillations revealed by sweeping the central gate voltage V_C of the Mach-Zehnder interferometer. A color plot of the current as a function of V_C and V_P is displayed in Fig. 3. This plot corresponds to experiments with five different drain-source voltages V_{DS}. One would expect a current injection only for a range of V_P values between 0 and V_{DS} (see the inset of Fig. 1), and this is indeed what can be seen in the top graph of Fig. 3, where the window of nonzero current (around 25 pA) increases linearly with increasing source-drain voltage. Sweeping V_C while V_P is within this window reveals the quantum interferences. The interference pattern is clearly observable in Fig. 3. It is easily noticed that, within the window for nonzero current, the amplitude
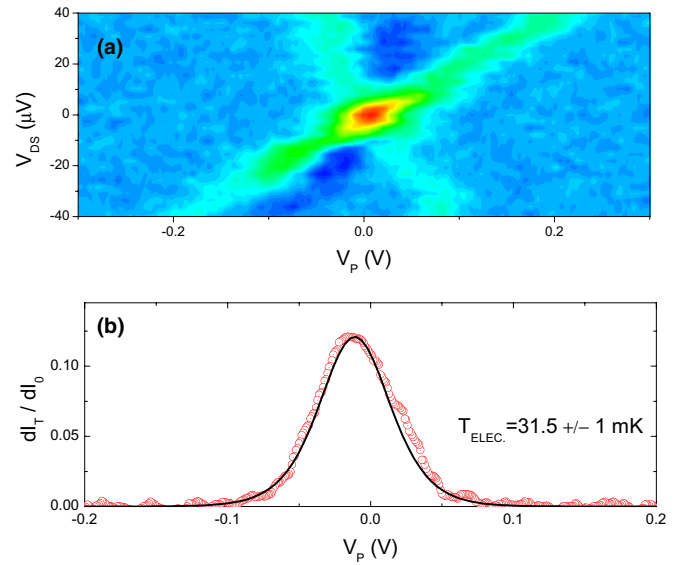

FIG. 2. (a) Color plot of the transmission probability through the quantum dot as a function of the plunger voltage V_P and the drain source voltage V_{DS}. (b) Transmission probability as a function of V_P at zero bias. The continuous line is a fit of this resonance.

of the current oscillations appears to change very little, a clear indication that the quantum interferences, and hence the coherence, are more or less independent of the injection energy of the electrons.

To be more quantitative, we plot in Fig. 4 the visibility $\frac{I_{\max} - I_{\min}}{I_{\max} + I_{\min}}$ of quantum interferences as a function of the injected energy. Surprisingly, for energies greater than 20 μeV, the visibility remains almost constant instead of decreasing down to zero as expected. We need to consider whether the saturation of the visibility is due to an unexpected robustness of the
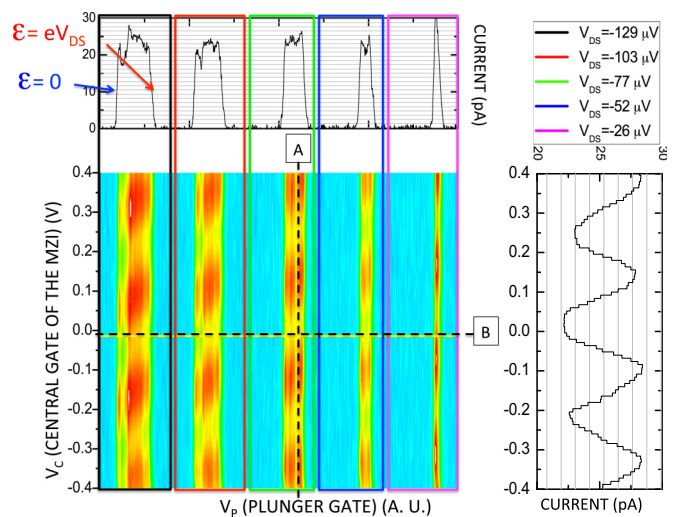

FIG. 3. Current as a function of the plunger gate voltage V_P and the central gate voltage V_C of the MZI for different values of the drain source bias V_{DS}. The top graph, representing the current as a function of V_P, corresponding to a 2D plot cut through line B. The right graph shows the interference pattern as a function of V_C corresponding to a cut through line A.
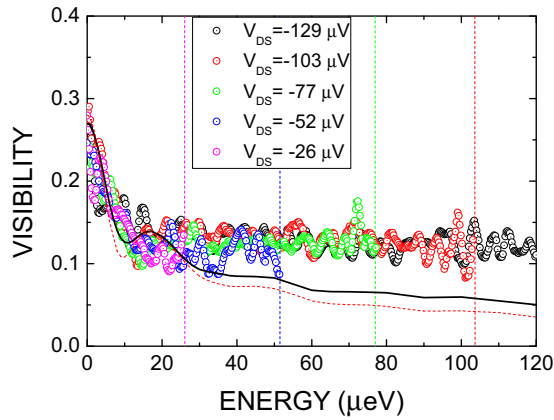
FIG. 4. Visibility of quantum interferences as a function of the energy for five different bias voltages. The vertical lines represent the maximum energy achievable for each bias. The solid and the dashed lines show the calculated visibility for interaction parameters $\theta = \pi/2$ and $\theta = \pi/3$, respectively.

quantum coherence, or e.g., to the finite distance, 2.7 μm, between the energy filter and the MZI. Indeed, a short relaxation length ($\ll 2.7$ μm) would mean that the electrons injected above the Fermi sea are fully relaxed before reaching the entrance of the interferometer. However, this scenario is in contradiction both with recent experimental results and theories, as we will now show.

On the experimental side, experiments at a filling factor of 2 with a hot electron distribution in one channel have demonstrated that the inelastic length is of the order of 3 μm [13]. This length is of the order of the separation between the QD and the MZI, meaning that electrons are only partially relaxed. A second experimental evidence against fast relaxation is the Hong-Ou-Mandel (HOM) experiment with electrons injected one by one into edge states via quantum dots, which are excited with a periodic radio-frequency gate voltage matched to their addition energy [3]. The observed HOM dip, resulting from the collision of two electrons emerging from two separate sources, implies a coherent propagation of the injected electrons. This observation, for which electrons have been injected at energies higher than 1 meV, shows qualitatively that an important fraction of the injected electrons remains coherent, as observed in our experiment.

Furthermore, our quantitative model calculations show that the electrons reaching the MZI are only partially relaxed. We describe our system through an approach similar to Ref. [22], which considers the relaxation of an energy resolved single electron wave packet $\phi_{k_0}(x) \propto e^{ik_0 x}$ injected in the outer edge channel, and takes into account the coupling of the $\nu = 2$ edge channels [4]. This approach has proved useful for the understanding of unexpected phenomena observed on out-of-equilibrium MZIs [17], and of the observed energy transfer between edge channels [13,23]. The coupling to the electromagnetic environment, responsible for the electronic decoherence, is described by an electrostatic coupling to a metallic electrode, itself connected to the ground by an arbitrary impedance at an arbitrary temperature. This idealized picture is expected to be valid for electrons having a typical

injection energy $\varepsilon_0 = \hbar v_F k_0 \gg \Delta\epsilon$, with $\Delta\epsilon$ their energy width. It is a criterion that is valid in our experiment, and as long as the dephasing environment can be considered as linear and in thermal equilibrium. Based on our previous experiments on phase coherence in the integer quantum Hall effect (IQHE) at $\nu = 2$ [11,12], we assume that the electromagnetic environment of the interfering edge state consists of the co-propagating edge state, which replaces the metallic gate. Furthermore, as we probe the phase coherence of electrons injected at energies above the Fermi sea much higher than the thermal energy, we assume a zero temperature of the neighboring edge mode. The effect of its finite temperature is then simply taken into account in the finite visibility of Aharonov-Bohm (AB) interferences at zero energy. The two main outcomes of this approach to quasiparticle relaxation are the electron distribution $\delta n(k, k_0, L)$ and the elastic scattering probability $\mathcal{Z}(k_0, L)$ after a finite propagation length L. The visibility is then obtained from $\int \delta n(k, k_0 L) \mathcal{Z}(2k_0 L) dk$.

To include the relaxation on the length L_{QD} separating the QD from the MZI, we computed $\delta n(k, k_0 L_{QD})$ and the full theoretical $\mathcal{V}_{Theo.} \propto \int \delta n(k, k_0 L_{QD}) \mathcal{Z}(2k L_{MZI}) dk$, where L_{MZI} is the MZI arm length. The inclusion of this length shows that the electronic wave packet is partially (and not totally) relaxed before entering the MZI. The theoretical results are plotted in Fig. 4 for two different values of the coupling parameter θ measured in recent experiments [24,25]. In order to fit our data and the decrease of the visibility at low energy, we chose a drift velocity of 5×10^4 ms^{-1}. However, the general appearance of the curves does not qualitatively change for reasonable values of the coupling strength and of the drift velocity (see SM [21]).

As expected, but in contradiction with our observations, the theory does not lead to a saturation of the visibility at high energy, but to a continuous decrease, albeit with a slope less pronounced than at low energy. This continuous decrease can be easily understood: For a short range interaction, the environment can absorb any energy; hence, the higher the injection energy, the larger is the probability for energy losses. This argument is in fact quite general and should apply regardless of the microscopic details of the model. Hence, although the other existing models [4,26–28] have not treated explicitly the decoherence of electrons injected in a narrow energy window above the Fermi level, we do not expect they would yield predictions qualitatively different from ours, as they also start from a short range Coulomb interaction between co-propagating edge channels. Last, a recent theoretical paper [29] based on short range interaction reaches the same conclusions. Our experimental observation of a saturation of the high energy visibility suggests the existence of another not yet identified energy scale in the system, or suggests the presence of an additional relaxation mechanism which remains to be identified. A somewhat similar effect has been probed at lower filling factors and much higher energies [30].

The robustness of the quantum coherence, which we have demonstrated here, increases the attraction of electron guns for quantum optics type experiments. At the same time, our results raise questions regarding our understanding of excitations in the integer quantum Hall regime. To further elucidate the relaxation in edge states, the next step in this experiment will be to implement a second

quantum dot after the MZI, to make the spectroscopy of the injected electron after its propagation through the interferometer.

[1] Y. Ji, Y. Chung, D. Sprinzak, M. Heiblum, D. Mahalu and H. Shtrikman, Nature (London) **422**, 415 (2003).

[2] G. Fève, A. Mahé, J.-M. Berroir, T. Kontos, B. Plaçais, D. C. Glattli, A. Cavanna, B. Etienne, and Y. Jin, Science **316**, 1169 (2007).

[3] E. Bocquillon, V. Freulon, J.-M Berroir, P. Degiovanni, B. Plaçais, A. Cavanna, Y. Jin, and G. Fève, Science **339**, 1054 (2013).

[4] I. P. Levkivskyi and E. V. Sukhorukov, Phys. Rev. B **78**, 045322 (2008).

[5] C. W. J. Beenakker, C. Emary, M. Kindermann, and J. L. van Velsen, Phys. Rev. Lett. **91**, 147901 (2003).

[6] P. Samuelsson, E. V. Sukhorukov, and M. Büttiker, Phys. Rev. Lett. **92**, 026805 (2004).

[7] G. Haack, M. Moskalets, J. Splettstoesser, and M. Buttiker, Phys. Rev. B **84**, 081303(R) (2011).

[8] G. Rosselló, F. Battista, M. Moskalets, and J. Splettstoesser, Phys. Rev. B **91**, 115438(R) (2015).

[9] R. C. Ashoori, H. L. Stormer, L. N. Pfeiffer, K. W. Baldwin, and K. West, Phys. Rev. B **45**, R3894 (1992).

[10] N. Kumada, H. Kamata, and T. Fujisawa, Phys. Rev. B **84**, 045314 (2011).

[11] P. Roulleau, F. Portier, D. C. Glattli, P. Roche, A. Cavanna, G. Faini, U. Gennser, and D. Mailly, Phys. Rev. Lett. **100**, 126802 (2008).

[12] P. Roulleau, F. Portier, P. Roche, A. Cavanna, G. Faini, U. Gennser, and D. Mailly, Phys. Rev. Lett. **101**, 186803 (2008).

[13] H. le Sueur, C. Altimiras, U. Gennser, A. Cavanna, D. Mailly, and F. Pierre, Phys. Rev. Lett **105**, 056803 (2010).

[14] I. Neder, M. Heiblum, Y. Levinson, D. Mahalu, and V. Umansky, Phys. Rev. Lett. **96**, 016804 (2006).

[15] P. Roulleau, F. Portier, D. C. Glattli, P. Roche, A. Cavanna, G. Faini, U. Gennser, and D. Mailly, Phys. Rev. B **76**, 161309(R) (2007).

[16] L. V. Litvin, H. P. Tranitz, W. Wegscheider, and C. Strunk, Phys. Rev. B **75**, 033315 (2007).

[17] P.-A. Huynh, F. Portier, H. le Sueur, G. Faini, U. Gennser, D. Mailly, F. Pierre, W. Wegscheider, and P. Roche, Phys. Rev. Lett. **108**, 256802 (2012).

[18] L. D. Landau, Sov. Phys. JETP **3**, 920 (1957).

[19] L. D. Landau, Sov. Phys. JETP **8**, 70 (1959).

[20] C. W. J. Beenakker, Phys. Rev. B **44**, 1646 (1991).

[21] See Supplemental Material at http://link.aps.org/supplemental/10.1103/PhysRevB.93.035420 for details on the Quantum Dot tuning as well as a longer explanation of the theoretical approach.

[22] P. Degiovanni, C. Grenier, and G. Fève, Phys. Rev. B **80**, 241307(R) (2009).

[23] P. Degiovanni, C. Grenier, G. Fève, C. Altimiras, H. le Sueur, and F. Pierre, Phys. Rev. B **81**, 121302(R) (2010).

[24] H. Inoue, A. Grivnin, N. Ofek, I. Neder, M. Heiblum, V. Umansky, and D. Mahalu, Phys. Rev. Lett. **112**, 166801 (2014).

[25] E. Bocquillon, V. Freulon, J.-M. Berroir, P. Degiovanni, B. Plaçais, A. Cavanna, Y. Jin, and G. Fève, Nat. Commun. **4**, 1839 (2013).

[26] L. Chirolli, F. Taddei, R. Fazio, and V. Giovannetti, Phys. Rev. Lett. **111**, 036801 (2013).

[27] M. J. Rufino, D. L. Kovrizhin, and J. T. Chalker, Phys. Rev. B **87**, 045120 (2013).

[28] C. Wahl, J. Rech, T. Jonckheere, and T. Martin, Phys. Rev. Lett. **112**, 046802 (2014).

[29] A. O. Slobodenisk, E. G. Idrisov, and E. V. Sukhorukov, Phys. Rev. B **93**, 035421 (2016).

[30] J. D. Fletcher, P. See, H. Howe, M. Pepper, S. P. Giblin, J. P. Griffiths, G. A. C. Jones, I. Farrer, D. A. Ritchie, T. J. B. M. Janssen, and M. Kataoka, Phys. Rev. Lett. **111**, 216807 (2013).